Title: **RAD Sequencing Enables Unprecedented Phylogenetic Resolution and Objective Species Delimitation in Recalcitrant Divergent Taxa**

Authors: Santiago Herrera[1,2]*, Timothy M. Shank[1]

[1]*Massachusetts Institute of Technology, Cambridge, MA, USA*

[2]*Biology Department, Woods Hole Oceanographic Institution, Woods Hole, MA, USA*

**Present affiliation: University of Toronto, Toronto, ON, Canada*

Email addresses: S. Herrera sherrera@alum.mit.edu; T.M. Shank tshank@whoi.edu

Corresponding authors: Santiago Herrera and Timothy M. Shank; 266 Woods Hole Road, MS33, Woods Hole, MA 02543, USA. Tel: +1 508 289 3761, Fax: +1 508-457-2134.

Abstract

Species delimitations is problematic in many cases due to the difficulty of evaluating predictions from species hypotheses. In many cases delimitations rely on subjective interpretations of morphological and/or DNA data. Species with inadequate genetic resources needed to answer questions regarding evolutionary relatedness and genetic uniqueness are particularly problematic. In this study, we demonstrate the utility of restriction site associated DNA sequencing (RAD-seq) to objectively resolve unambiguous phylogenetic relationships in a recalcitrant group of deep-sea corals with divergences >80 million years. We infer robust species boundaries in the genus *Paragorgia* by testing alternative delimitation hypotheses using a Bayes Factors delimitation method. We present substantial evidence rejecting the current morphological species delimitation model for the genus and infer the presence of cryptic species associated with environmental variables. We argue that the suitability limits of RAD-seq for phylogenetic inferences cannot be assessed in terms of absolute time, but are contingent on taxon-specific factors. We show that classical taxonomy can greatly benefit from integrative approaches that provide objective tests to species delimitation hypotheses. Our results lead the way for addressing further questions in marine biogeography, community ecology, population dynamics, conservation, and evolution.

Keywords

Cryptic species; Species delimitation; BFD*; Phylogenomics; SNPs; RAD-seq.

1. Introduction

Species delimitation is problematic in many taxa due to the difficulty of evaluating predictions from species hypotheses derived using different species concepts. Species concepts set particular expectations of the properties used to support species delimitations (De Queiroz, 2007). For example, the classic biological species concept requires intrinsic reproductive isolation between heterospecific organisms and interbreeding among homospecific organisms resulting in viable and fertile descendants (Mayr, 1942). In many, if not the majority of cases, it is difficult to evaluate behavioural, reproductive, and ecological properties due to technical limitations of field or laboratory work, which largely determine the kind of observations and data that can be obtained. In these cases researchers conventionally rely on morphological observations and/or DNA sequence data to generate species delimitation hypotheses.

Although there have been significant attempts to develop statistical methods that objectively identify species-diagnostic morphological discontinuities (e.g., Zapata and Jimenez 2012), many species delimitations are performed subjectively based on assessments made by specialized taxonomists. Molecular phylogenetic analyses of DNA sequences provide independent means to test these species delimitation hypotheses utilizing a variety of methods, ranging from variability thresholds of barcode sequences (Hebert et al., 2003) to probabilistic coalescent-based model methods (Fujisawa and Barraclough, 2013; Yang and Rannala, 2010). These molecular methods rely on informative DNA sequence markers, and in many cases on resolved phylogenies.

The sub-class Octocorallia (Phylum Cnidaria), which includes animals known as

61 gorgonians, sea pens, and soft corals, is an example of a recalcitrant group wherein species
62 delimitations are problematic. Octocorals are predominantly a deep-sea group (Cairns, 2007;
63 Watling et al., 2011) and therefore are extremely difficult to observe and collect. Classic
64 morphology-based species delimitation and identification in this group is arduous for non-
65 specialists, and challenging to replicate among taxonomists (Catherine S. McFadden et al.,
66 2010b). Variations in octocoral colony architecture and micro-skeletal structures – sclerites – are
67 used as species diagnostic characters (e.g. Bayer, 1956). However, studies over the last 15 years
68 have shown that in many cases species delimitations and systematics based on these
69 morphological traits keep little to no correspondence with the patterns of genetic diversity and
70 relatedness inferred using mitochondrial and ribosomal DNA sequence markers (Dueñas and
71 Sánchez, 2009; France, 2007; McFadden et al., 2006). A confounding factor when analysing
72 mitochondrial DNA markers is the fact that anthozoans, including octocorals, have slow rates of
73 sequence evolution relative to other metazoans (Hellberg, 2006; Shearer et al., 2002).
74 Furthermore, octocoral mitochondrion is unique among eukaryotes by having a functional DNA
75 mismatch repair gene — *mtMutS* — which presumably is responsible for the extremely low
76 sequence variability observed in this group (Bilewitch and Degnan, 2011). Traditional molecular
77 markers have thus been remarkably insufficient to resolve relationships at all taxonomic levels
78 within the octocorals (Catherine S. McFadden et al., 2010b). Alternative nuclear markers, such
79 as the ITS2 and *SRP54* have been used to examine interspecific and intraspecific relationships
80 (Aguilar and Sánchez, 2007; Concepcion et al., 2007; Herrera et al., 2010); however, their
81 application and impact has been limited due to issues regarding intragenomic variability
82 (Sánchez and Dorado, 2008) and low sequencing reliability (Catherine S. McFadden et al.,
83 2010a). These long-standing technical problems have caused fundamental questions in

84 octocorals regarding species differentiation, systematics, diversity, biogeography, community
85 ecology, population dynamics, and evolution to remain unanswered.
86
87 Technological developments in next-generation sequencing platforms and library
88 preparation methodologies have made genomic resources increasingly accessible and available
89 for the study of non-model organisms, thus offering a great opportunity to overcome the
90 difficulties inherent to the use of traditional sequencing approaches. One of these methodologies
91 is restriction-site-associated DNA sequencing (RAD-seq), which combines enzymatic
92 fragmentation of genomic DNA with high-throughput sequencing for the generation of large
93 numbers of markers (Baird et al., 2008). RAD-seq has shown great promise to resolve difficult
94 phylogenetic, phylogeographic, and species delimitation questions in diverse groups of
95 eukaryotes (Cruaud et al., 2014; Emerson et al., 2010; Herrera et al., 2015b; Leaché et al., 2014;
96 Wagner et al., 2012) , including cnidarians (Reitzel et al., 2013) and most recently deep-sea
97 octocorals (Pante et al., 2014). The number of orthologous restriction sites that can be retained
98 across taxa, which decreases as divergence increases, limits the usefulness of RAD-seq for these
99 kinds of studies. *In silico* studies in model organisms indicate that RAD-seq can be used to infer
100 phylogenetic relationships in young groups of species (up to 60 million years old), such as
101 *Drosophila* (Cariou et al., 2013; Rubin et al., 2012)*;* however, the boundary limits of this
102 technique have only been empirically explored in a handful of mostly younger groups (Cruaud et
103 al., 2014; Gonen et al., 2015; Hipp et al., 2014; Leaché et al., 2015).
104
105 In this study, we aim to empirically explore the limits of RAD-seq to solve questions in
106 phylogenetics and species delimitation. We focus on the recalcitrant *Anthomastus-Corallium*

clade of octocorals (*sensu* McFadden et al. 2006) to test the utility of RAD-seq to resolve phylogenetic relationships among divergent taxa, and to infer objective species boundaries. Corals in the *Anthomastus-Corallium* clade (hereafter referred as the AC clade) are among the most conspicuous, widely distributed, and ecologically important benthic invertebrates in deep-water ecosystems (Roberts et al., 2009). This clade is constituted by more than 100 species defined morphologically, divided in 10 genera, and three families (World Register of Marine Species at http://www.marinespecies.org accessed on 2014-10-10), spanning a divergence time of over 100 million years (Ardila et al., 2012; Herrera et al., 2012). However, species delimitations and phylogenetic relationships in this clade, as in other octocorals, are controversial and conflictive (Ardila et al., 2012; Herrera et al., 2012, 2010). Many of the species in this group are considered species indicators of Vulnerable Marine Ecosystems (ICES, 2013), with some of them considered endangered (CITES, 2014). Accurate species identifications, as well as complete inventories and knowledge of species ranges, are therefore critical to ensure the effectiveness and appropriateness of conservation and management policies.

2. Materials & methods

2.1. *Morphological species identifications and DNA sequencing*

To carry out identifications using current morphological coral species descriptions, we performed scanning electron microscopy of sclerites on 44 octocoral specimens from the AC clade (Table S1) identifying 12 putative morphospecies. To obtain a dense genome-wide set of markers we performed RAD sequencing with the 6-cutter restriction enzyme PstI (using PredRAD (Herrera et al., 2015a) we predicted between 32,000-110,000 cleavage sites in their

genomes [Table S2]). DNA was purified following (Herrera et al., 2015b). Concentration-normalized DNA was submitted to Floragenex Inc (Eugene, OR) for library preparation and RAD sequencing. Libraries were sequenced by 48-multiplex, using 10-base pair barcodes, on a lane of Illumina Hi-Seq 2000 (100bp). This yielded 3.9 ± 1.4 million raw reads (average ± standard deviation) per individual. To compare the inferences obtained from RAD-seq data with the inferences drawn from traditional genetic barcoding data, we performed Sanger sequencing of the mitochondrial *mtMutS* gene on the same specimens. PCRs were carried out following (Herrera et al., 2015b), with primers described by (Herrera et al., 2010), and sequencing was performed by Eurofins Genomics (Eurofins MWG Operon, Inc.)

2.2. *RAD-seq data filtering clustering and phylogenetic inference*

Sequence reads were de-multiplexed and quality filtered with the *process_radtags* program from the package Stacks v1.20 (Catchen et al., 2013) using the following parameters: *-t* 91, *-c*, *-s* 10, *-r*, and *-w* 0.15. Additional filtering, and the clustering within and between individuals to identify homologous loci (full sequences, including invariable sites and single nucleotide polymorphisms) was performed using the program pyRAD v2.01 (Eaton, 2014). Approximately 74.3 ± 8.1% of the raw reads were retained after these steps (Table S3). To examine the sensitivity of the phylogenetic inference to the clustering parameters used to identify orthologous loci and create nucleotide matrices in pyRAD, we investigated different combinations of clustering thresholds (*c* 0.80, 0.85 and 0.90) and minimum number of taxa per locus (*m* 4, 6, and 9) in a set of **'backbone'** supermatrices containing one individual from each of the 12 identified morphospecies. The minimum depth of coverage required to build a cluster and the maximum number of shared polymorphic sites in a locus were kept constant at 4 (*d*) and

153 3 (*p*) respectively. The 9 resulting **backbone** supermatrices ranged in the total number of loci per
154 matrix from ~9 to 60 thousand loci, increasing dramatically as the minimum number of taxa per
155 locus was reduced (Table S4). In contrast, the different clustering thresholds did not have a
156 significant effect on the total number of loci, but rather on the number of variable sites and, most
157 importantly, on the number of phylogenetically-informative sites (Table S4). Each of the
158 resulting **backbone** supermatrices was analysed in RAxML-HPC2 v8.0 (Stamatakis, 2014) for
159 maximum likelihood (ML) phylogenetic inference. For this, and all the other phylogenetic
160 analyses in RAxML, we assumed the GTR GAMMA substitution model as suggested by the
161 Akaike Information Criterion (AIC) implemented in JModelTest 2.0 (Darriba et al., 2012).
162 Branch support was assessed by 500 bootstrap replicates.
163
164 We selected an optimal combination of loci clustering parameters as the set of parameters
165 that minimized the number of missing data and maximized the number of phylogenetically-
166 informative sites while producing a highly supported phylogenetic tree. These optimal
167 parameters were: clustering threshold of 80% similarity among sequences (*c* 0.80) and a
168 minimum coverage of taxa per locus of 75% (*m* 9) (Table S4). The resulting supermatrix had
169 20% missing data, and 24% of the variable sites were phylogenetically-informative. A
170 supermatrix containing the sequence data of all the 44 octocoral specimens, denominated
171 **'PHYLO',** was built using this parameter combination (*c* 0.80, *m* 33) in pyRAD (see Table S5
172 for individual statistics) and analyzed in RAxML. This supermatix has 5,997 loci with 85,293
173 variable sites; 53,150 of which were phylogenetically informative.
174
175 **2.3. *Phylogenetic inference with traditional genetic barcoding data***

176 To compare the tree topology obtained from the phylogenetic inferences of the **PHYLO**
177 supermatrix with traditional genetic barcoding data we analyzed the *mtMutS* sequences from the
178 same individuals (hereafter referred to as **'mitochondrial'** matrix) using RAxML. To place the
179 specimens from this study in a broader phylogenetic context we added data from 233 additional
180 specimens belonging to the AC clade, as well as outgroups, to the **mitochondrial** matrix (see
181 Table S6, Figs. S2 and S3), and analyzed it with RAxML.
182
183 **2.4. *Testing species delimitation models for Paragorgia***
184 To evaluate the utility of RAD-seq to perform objective species delimitations in
185 octocorals we focused on specimens of the genus *Paragorgia* – the best-sampled taxon in our
186 dataset, both in terms of geographic representation and number of putative morphospecies. We
187 used the Bayes Factor Delimitation method with genomic data (BFD*) (Leaché et al., 2014),
188 which allows for the comparison of alternative species delimitation models in an explicit
189 multispecies coalescent framework using genome-wide SNP data. We calculated marginal
190 likelihood estimates (MLE) of alternative taxonomy-informed and taxonomy-independent
191 species delimitation models on a supermatrix of unlinked SNPs from the 31 specimens of
192 *Paragorgia* (**'PARAGORGIA'**: *c* 0.80, and *m* 31 for 0% missing data; only one SNP per locus,
193 for a total of 1,203 SNPs), and compared them to the MLE of the null model '**morphid'**, which
194 is based on current morphological species descriptions (Sánchez, 2005). MLE were obtained
195 using the implementation of BFD* in the SNAPP (Bryant et al., 2012) plug-in for BEAST v2.1.3
196 (Bouckaert et al., 2014). We performed a path-sampling of 48 steps (MCMC length 100,000,
197 pre-burnin 10,000), following (Leaché et al., 2014). Bayes Factors (BF) were calculated from the
198 MLE for each model and compared (Kass and Raftery, 1995).

199

200 Four alternative taxonomy-informed species delimitation models were defined for
201 *Paragorgia*: **i**) '**PAB'**: **morphid** plus a split of *P. arborea* based on previous evidence of genetic
202 differentiation of north Pacific populations (Herrera et al., 2012); **ii**) '**STE'**: **morphid** plus a split
203 of *P. stephencairnsi* based on depth differences (specimens collected <350m vs. >1000m), as
204 depth is known to be an important structuring variable in marine taxa (Jennings et al., 2013;
205 Prada and Hellberg, 2013; Quattrini et al., 2015); **iii**) '**PABSTE'**: **morphid** plus the splits of
206 **PAB** and **STE**; and **iv**) '**splitPAB'**: **morphid** plus the split of **STE** and an additional split in
207 **PAB** where *P. arborea* is split in 3 corresponding to the ocean basin where the specimens were
208 collected (north Pacific, south Pacific and north Atlantic).
209

210 Five alternative taxonomy-independent models for *Paragorgia* were defined through
211 Bayesian and ML implementations of the Poisson tree processes model (PTP) (available at
212 http://species.h-its.org/ptp/). PTP estimates the number of speciation events in a rooted
213 phylogenetic tree in terms of nucleotide substitutions (Zhang et al., 2013). We used PTP to
214 analyse the trees obtained from ML phylogenetic inferences of reduced **mitochondrial** and
215 **PHYLO** matrices that included the 33 specimens from the family Paragorgiidae (genera
216 *Paragorgia* and *Sibogagorgia*) exclusively. The '**PARAGORGIIDAE'** RAD-seq supermatrix
217 was generated in pyRAD (*c* 0.80 and *m* 33; this supermatix has 446 loci with 3,595 variable
218 sites; 2,361 of which were phylogenetically informative). The resulting trees were rooted with
219 *Sibogagorgia* and analyzed by the PTP method (MCMC length 500,000, 100 thinning, 25%
220 burnin). We assessed convergence by examining the likelihood trace. The combinations of ML
221 and Bayesian PTP implementations (mlPTP and bPTP) with the **PARAGORGIIDAE** *mtMutS*

and RAD-seq trees resulted in four species delimitation models: **'mlPTP*mt*'**, **'bPTP*mt*'**, **'mlPTPrad'**, and **'bPTPrad'**. Lastly, because deep-sea corals are known to show genetic differentiation at ocean basin/regional scales (Herrera et al., 2012; Miller et al., 2011; Morrison et al., 2011), we constructed an additional taxonomy-uninformed naïve species delimitation model, '**geo',** based on the geographic location where the specimens were collected (north Pacific, south Pacific or north Atlantic ocean basins). A extreme model were all *Paragorgia* specimens were part of a single species was tested, however the probability of this model given the data was extremely small, approaching 0, which caused a computational logic error in all attempts (data not shown).

2.5. *Species tree inference*

To test the tree topology in the genus *Paragorgia* obtained by the phylogenetic analysis of the **PHYLO** and **PARAGORGIIDAE** concatenated supermatrices we performed a species tree inference from the SNP data in the **PARAGORGIA** matrix using SNAPP. This program allows the inference of species trees from unlinked SNP data while bypassing the inference of individual gene trees. We performed 3 independent runs (MCMC length 10,000,000; sampling every 1,000; pre-burnin 1,000) with default priors for coalescence rate, mutation rate and ancestral population size parameters. We assessed convergence to stationary distributions and effective sample sizes >200 after 10% burnin in TRACER (Rambaut and Drummond, 2007). Species trees in the posterior distribution were summarized with DENSITREE v2.01 (Bouckaert, 2010).

3. Results & discussion

3.1. *RAD sequencing enables unprecedented phylogenetic resolution*

Our analyses of RAD-seq data provide a robust and fully resolved phylogenetic hypothesis for the recalcitrant octocorals in the *Anthomastus-Corallium* clade, a result never achieved before. This study together with the work by Pante et al. (2014) in the octocoral genus *Chrysogorgia*, constitute the first applications of RAD-sequencing for phylogenetics and species delimitation in cnidarians, and one of the first ones in invertebrates. All of our analyses based on RAD-seq supermatrices – varying in taxon coverage, degree of divergence among taxa, proportion of missing data, number of loci, and analysis type (ML concatenated loci or Bayesian SNPs species tree) – produced completely congruent and strongly supported trees, which together provide extremely high confidence on the phylogenetic hypothesis inferred for the octocoral AC clade (Figs. 1, 2, 3, 4 and Fig. S1). Each one of the morphologically identified families, genera, and species in this dataset were monophyletic. The branching pattern of the tree is consistent with an expected transition between coalescent processes among species and genera (long deep branches), and population processes within species (short shallow branches).

3.2. *Single markers alone can produce biased phylogenetic inferences*

Only a handful of studies, using traditional mitochondrial data and the ITS2 and 28S nuclear markers, have attempted to evaluate phylogenetic relationships in the octocoral AC clade (Ardila et al., 2012; Figueroa and Baco, 2015; Herrera et al., 2012, 2010; McFadden and van Ofwegen, 2013; Uda et al., 2013). These studies find support for the monophyly of the genus *Paragorgia,* the family Coralliidae, and the sister relationship between the Paragorgiidae and Coralliidae. However, those data do not provide enough phylogenetic resolution to infer the evolutionary relationships among many of the putative morphological species. Furthermore,

269 significant incongruences between mitochondrial and nuclear ITS2 gene trees from AC taxa have
270 been documented by (Herrera et al., 2010). Here we reproduce similar incongruences in tree
271 topology when comparing the trees inferred from mitochondrial and nuclear RAD-seq datasets
272 (Fig. 2). Likewise, Pante et al. (2014) documented marked incongruence between trees inferred
273 from mitochondrial and RAD-seq data in *Chrysogorgia.* These observations suggest that
274 processes that can cause gene tree heterogeneity, such as incomplete lineage sorting and
275 horizontal gene transfer (Edwards, 2009; Maddison, 1997), may be more prevalent in octocorals
276 than previously recognized. Consequently, we suggest that single marker gene trees in octocorals
277 and other taxa, particularly from the mitochondria (including whole mitochondrial genomes),
278 should not be considered as robust hypotheses of true species phylogenies on their own, without
279 further validation by multiple informative and independent nuclear loci. While we recognize the
280 important utility of using single barcoding gene regions for the rapid assessment of species
281 assignments, we urge systematists to be conservative when making taxonomic rearrangements
282 based on inferences from single-marker data alone.
283
284 **3.3. *RAD-seq data is suitable for phylogenetic inference in divergent taxa***
285 Contrary to the currently accepted idea that RAD-seq data are only suitable for taxa with
286 divergence times younger than 60 million years (MY) (Rubin et al., 2012), we demonstrate their
287 suitability well beyond this age threshold. Remarkably, we were able to confidently resolve
288 phylogenetic relationships among genera from different families diverging by at least 80 MY in
289 the AC clade. The split between the lineages leading to the families Paragorgiidae and
290 Coralliidae has been dated, using coralliid fossils, to be between 80-150 MY old (Ardila et al.,
291 2012; Herrera et al., 2012). We found that the proportion of shared loci among individuals from

292 these to families in our optimal **backbone** supermatrix was 70-80% (Fig. 1). Park et al. (2012)
293 estimated the age of the most recent common ancestor of the Coralliidae at approximately 50
294 MY (25-100 MY 95% confidence region), using independent cnidarian fossils for molecular
295 clock calibration. The split with the genera *Anthomastus* and *Heteropolypus* is likely older than
296 100 MY. It is without question that, due to mutation at restriction sites, the number of RAD loci
297 among taxa for which orthology can be established decreases rapidly as divergence increases.
298 However, we suggest that the suitability limits of RAD-seq for phylogenetics in divergent taxa
299 cannot be assessed in terms of absolute time, but depend on taxon-specific factors such as
300 mutation rate, generation time and effective population size.
301
302 Bioinformatic studies addressing the issue of extent of the suitability of RAD-seq for
303 phylogenetic inference have focused mainly on *Drosophila* as a study model (Cariou et al., 2013;
304 Rubin et al., 2012). Longer generation times and lower metabolic rates in taxa like deep-sea
305 corals, relative to those in organisms like *Drosophila,* could cause a reduction in mutation rates
306 (see review by Baer et al. (2007)), which may in turn decrease the evolutionary rates at
307 restriction sites and allow for phylogenetic inferences using RAD-seq in situations of deeper
308 divergence. Consistent with this hypothesis, we observe a nucleotide diversity (π) calculated
309 across all octocoral specimens from the **PHYLO** matrix of 0.012 ± 0.002 (considered a
310 minimum since RAD-seq data can lead to diversity underestimates (Arnold et al., 2013) (see
311 Table S7 and Table S8 for individual values), which is significantly lower than the nucleotide
312 diversity in many of the *Drosophila* species (Cariou et al., 2013; Rubin et al., 2012). In addition
313 to mutation rates and nucleotide diversity, there are many factors and processes known to
314 influence genetic diversity across species – and likely the evolutionary rate as well. These factors

include the effective population size, selection, habitat, geographic range, and mating system (Leffler et al., 2012). We suggest that the cumulative expression of these processes are captured by RAD-seq approaches and can be successfully used to infer phylogenetic relationships in certain taxa with deeper divergences than previously suggested. This is particularly true when the number of RAD loci is maximized through the choice of restriction enzymes with higher cutting frequencies in the target taxon (Herrera et al., 2015a).

3.4. *RAD-seq reveals cryptic diversity and allows robust species delineations*

Our study, a statistically-rigorous genomic test of species hypotheses in octocorals, provides substantial evidence rejecting the current morphological species delimitation model for the genus *Paragorgia*. Branch-length differences among individuals, as well as well-supported sub-clades, revealed intraspecific genetic diversity that was undetected by the **mitochondrial** matrix. Furthermore, we find very strong support from Bayes Factors (2log(BF)>10; *sensu* Kass and Raftery, 1995) for a nested model (**PABSTE)** that combines species boundaries from morphological taxonomy with cryptic diversity linked to environmental variables of geographic location and depth (Figs. 3 and 4). The **PABSTE** model proposes 9 species among the examined specimens. Five of these species correspond to the morphological species *P. coralloides, P. kaupeka, P. alisonae, P. johnsoni,* and *P. maunga.* Two splits, corresponding to sub-clades in the morphological species *P. arborea* and in *P. stephencairnsi*, indicate cases of cryptic species.

Herrera et al. (2012) found significant genetic differentiation of the north Pacific populations of *P. arborea* relative to the south Pacific, Atlantic and Indian Ocean populations, and suggested that these populations likely represent sub-species. The north Pacific populations

of *P. arborea* were previously defined as a separate species, *P. pacifica,* by Verrill (1922) based on gross colony morphology, but later combined into a single species by Grasshoff (1979). Sánchez (2005) suggested potential small differences in medullar sclerite sizes and ornamentation between north Pacific specimens and specimens from elsewhere. However, we were unable to recognize these morphological differences in the few examined specimens in this study, which may reflect on the plasticity of these characters. Nonetheless, based on the very strong support for the split of *P. arborea* from analysis of genome-wide SNP makers, corresponding to a pattern of segregation by geographic location, we resurrect the species *Paragorgia pacifica* Verrill 1922 for the north Pacific populations of formerly *P. arborea*. We find no evidence of cryptic speciation between the north Atlantic and south Pacific *P. arborea* and therefore conclude it should be considered a single species as previously suggested by Herrera et al. (2012).

Depth is an important factor contributing to genetic differentiation and the formation of marine species living in shallow waters (Carlon and Budd, 2002; Prada and Hellberg, 2013) and at depth (Glazier and Etter, 2014; Jennings et al., 2013; Quattrini et al., 2013). The observed cryptic differentiation between specimens of *P. stephencairnsi* collected shallower than 350m and deeper than 1000m indicates that depth is also a diversifying force in octocorals from the AC clade, which had previously gone undetected (Herrera et al., 2012). The holotype of *P. stephencairnsi* was collected from approximately 350m in the Georgia Strait of British Columbia, overlapping in depth range and geographic region with that of most of the specimens from the shallow sub-clade examined in this study. Therefore, we propose to conserve that name

P. stephencairnsi for that shallow sub-clade, and consider the deep sub-clade as a new species *Paragorgia jamesi* sp. nov.

Family **Paragorgiidae** Kükenthal, 1916

Genus ***Paragorgia*** Stiasny, 1937

Paragorgia stephencairnsi species-complex

Revised morphological diagnosis [emended from Sánchez (2005)]: Robust branches. White, pink or red cortex; white or pink medulla; white, pink, red or purple autozooid apertures. Numerous conical, semi-closed, autozooid polyp apertures uniformly/randomly distributed throughout the branches. Siphonozooid apertures tightly closed, not observable to the naked eye. Medulla in the terminal branches with 6–7 major canals. Surface sclerites mostly 7- and 8-radiates, with long (> 0.01 mm) lobulated, smooth rays. Medulla with elongated, forked or irregular spindles, highly ornated, usually less than 0.3 mm in length.

***Paragorgia jamesi* sp. nov.**

Material examined: **Holotype** Royal British Columbia Museum (RBCM) 010-00234-004 (2344), TC2004-039 (Fig. 5 A-F); Latitude: 53.3709, Longitude: -133.3123; Depth: 1192-1195 m; Locality: Haida Gwaii, off Rennell Sound, west of Graham Island, British Columbia (BC), Canada; Collection date: 3 September 2001; Collector: Jim Boutillier. **Paratype** U.S. National Museum of Natural History (USNM) 1007316 (Fig. 5 G-K); Latitude: 48.4375, Longitude: -126.384; Depth: 1168 m; Locality: continental slope southwest of Vancouver Island, BC, Canada; Collection date: 9 September 2004; Collector: Jim Boutillier.

Diagnosis: Morphology as described for the species complex. *P. jamesi* (deep sub-clade) is differentiated from *P. stephencairnsi* (shallow sub-clade) by 125 fixed SNPs identified from the **PARAGORGIA** supermatrix (see Supplementary File 1 for details). *A posteriori* comparisons of morphological characters revealed that the lobulated rays of 7- and 8-radiate surface sclerites in *P. jamesi* have mostly rounded edges, whereas the ones from *P. stephencairnsi* have mostly sharp edges (Figs. 5 & 6).

Distribution: Northeaster Pacific Ocean. Continental slope off British Columbia, Canada. Depth range: 1168-1195 m.

Etymology: Named in honour of James David Rodríguez Rubio, arguably the best Colombian professional football (soccer) player in history. His many achievements were a source of inspiration for this work.

Remarks: The lobulated rays of 7- and 8-radiate surface sclerites of the paratype of *P. stephencairnsi* are mostly rounded [see Sánchez (2005) Fig. 41], resembling those of *P. jamesi* (Figs. 5 & 6). This specimen was also collected deeper than the range of all other *P. stephencairnsi* specimens (490 m). Thus it is likely that the paratype of *P. stephencairnsi* is a specimen of *P. jamesi*. However, the DNA from both the museum holotype and paratype of *P. stephencairnsi* was unsuitable for RAD-sequencing (degraded DNA or formalin fixation) and the proposed species designation could not be tested. Targeted SNP genotyping could help resolve this issue.

Paragorgia stephencairnsi *sensu stricto* Sánchez, 2005

Paragorgia stephencairnsi Sánchez 2005: 57.

406 **Holotype** USNM 57982; Latitude: 49.2307, Longitude: -123.74; Depth: 350 m; Locality:
407 4 miles northeast of Entrance Island, Strait of Georgia, BC, Canada; Collection date: 14 August
408 1973; Collector: Neil McDaniel. **Paratype** USNM 94437; R/V *Atlantis* AII-125, DSR/V *Alvin*
409 AD2296; Latitude: 32.4333, Longitude: -127.793; Depth: 490 m; Locality: Fieberling Guyot,
410 West Of Channel Islands, California (CA), USA; Collection date: 16 October 1990. Collector:
411 Lauren Mullineaux.
412 New material examined (see Table S1 for details): USNM 11224300 (OC 06); R/V
413 *McArthur II*; 188 m: off Ohiat Island, BC, Canda USNM 1157074 (101010, DW-026-02-6); R/V
414 *Velero IV*; 283 m; Piggy Bank, CA, USA. Woods Hole Oceanographic Institution (WHOI)
415 Agam, C02, C03, C04 & C05; Scuba; 32-41 m; Agamemnon Channel, BC, Canada. WHOI
416 C100-102 & C104; Scuba; 40 m; Tahsis Inlet, BC, Canada. Fisheries and Oceans Canada
417 (FOC)/WHOI FOC5 (5, 2009-47/ 71167), FOC25 (25, 2012-65/ 72750), FOC26 (26, 2012-65/
418 72750) & FOC30 (30, 2012-65/ 72750); 201-318 m; off Graham Island, BC, Canada.
419 Emended diagnosis: Morphology as described for the species complex. *P. stephencairnsi*
420 (shallow sub-clade) is differentiated from *P. jamesi* (deep sub-clade) by 125 fixed SNPs
421 identified from the PARAGORGIA matrix (see Supplementary File 1 for details). *A posteriori*
422 comparisons of morphological characters revealed that the lobulated rays of 7- and 8-radiate
423 surface sclerites in *P. stephencairnsi* have mostly sharp edges, whereas the ones from *P. jamesi*
424 have mostly rounded edges (Figs. 5 & 6).
425 Emended distribution: Northeaster Pacific Ocean. Continental shelf, shelf slope and
426 seamounts off California, USA to British Columbia, Canada. Depth range: 32-350 m.

Remarks: Holotype was collected from a submerged power cable that traversed the Strait of Georgia, British Columbia, from Point Grey to Nanaimo. The cable was being recovered because it was no longer being used but was valuable due to its core of solid copper.

***Paragorgia pacifica* Verrill 1922**

Paragorgia pacifica Verrill 1922: G16.

Paragorgia arborea: Sánchez 2005: 15.

New material examined (see Table S1 for details): RBCM 011-00067-002; off BC, Canada. RBCM 011-00160-001; off BC, Canada. USNM 1007340; 1168 m; off Vancouver Island, BC, Canada.

Emended diagnosis: Morphology as described by Sánchez (2005). This shallow sub-clade is differentiated from the deep sub-clade by 175 fixed SNPs identified from the PARAGORGIA matrix (see Supplementary File 2 for details).

Emended distribution: Northern Pacific Ocean. Continental shelf, shelf slope and seamounts off US and Canada west coast, from California to Alaska, Gulf of Alaska, Aleutian Islands, Bering Sea, Sea of Okhotsk and the Sea of Japan. Depth range: 15-1600 m.

Remarks: Herrera *et al.* (2012) found a conspicuous break in the genetic composition (mitochondrial haplotypes and nuclear ITS2) of *P. pacifica* between western and eastern North Pacific sub-regions, separated by the Alaska Peninsula. Whether these constitute isolated populations of *P. pacifica* or different cryptic species remains an open question.

4. Conclusions

In this case study we demonstrate the empirical utility of RAD-seq to resolve phylogenetic relationships among divergent and recalcitrant taxa and to objectively infer species boundaries by testing alternative delimitation hypotheses. We were able to make use of RAD-seq to overcome long-standing technical difficulties in octocoral genetics, and resolve fundamental questions in species definitions and systematics. We show that classic morphological taxonomy can greatly benefit from integrative approaches that provide objective tests to species delimitation hypotheses. Our results can serve as a guide for addressing rapidly-evolving hypotheses and fundamental questions in biogeography, species ranges, community ecology, population dynamics and evolution of recalcitrant taxa. The results from this study also represent a valuable reference resource for the development of tools, such as SNP arrays, that can be used to perform accurate species identifications, and generate species inventories that will aid the design and implementation of conservation and management policies.

Acknowledgements

This research was supported by the National Geographic Society/Waitt Foundation (W285-13 to SH); the National Oceanic and Atmospheric Administration (NOAA NA09OAR4320129 to TS); the National Science Foundation (NSF OCE-1131620 to TS); the National Aeronautics and Space Administration (NASA NNX09AB76G to TS); and the Academic Programs Office (Ocean Ventures Fund to SH), the Ocean Exploration Institute (Fellowship support to TMS) and the Ocean Life Institute of the Woods Hole Oceanographic Institution (WHOI).

For enabling access to key specimens we thank K. Schnabel, S. Mills, D. Tracey, M. Clark, A. Rowden, S. Cairns, E. Cordes, A. Quattrini, G. Workman, M. Wyeth, K. Anderson, M. Frey, H. Gartner, J. Boutillier, L. Watling, J. Adkins. We thank P. Aldersdale, N. Ardila and J. Sánchez for assistance with morphological identifications. We also thank V. Tunnicliffe, E. O'Brien, D. Forsman, J. Fellows, N. McDaniel, S. Schooner, J.Schooner and K. Helyar for assistance during scuba diving fieldwork in BC (DFO license FIN130270). We thank the chief scientists, masters, crew, scientific personnel, and funding agencies of expeditions AT07-35, KOK0506, Lophelia II 2009, RB-0503, TAN1007, TAN1104, TAN1206, and TAN1213. Specimens provided by the National Institute of Water and Atmospheric Research (NIWA) were collected under research programs: Kermadec Arc Minerals, funded by the New Zealand (NZ) Ministry of Business, Innovation & Employment (MBIE), Auckland University, Institute of Geological and Nuclear Science (GNS), and WHOI; Ocean Survey 20/20 funded by Land Information NZ; Impact of resource use on vulnerable deep-sea communities (CO1X0906), funded by MBIE; Nascent Inter-Ridge Volcanic And Neotectonic Activity, funded by the Ministry for Primary Industries (MPI), GNS, MBIE, and UNH; Scientific Observer Program funded by MPI; and the Joint NZ-USA 2005 NOAA Ring of Fire Expedition, part of NIWA's Seamount Program (FRST CO1X0508). We thank A.M. Tarrant, A.M. Reitzel, S. Edwards (editor) and two anonymous reviewers for providing helpful comments that improved this manuscript.

References

Aguilar, C., Sánchez, J.A., 2007. Phylogenetic hypotheses of gorgoniid octocorals according to ITS2 and their predicted RNA secondary structures. Mol. Phylogenet. Evol. 43, 774–786. doi:10.1016/j.ympev.2006.11.005

Ardila, N.E., Giribet, G., Sánchez, J.A., 2012. A time-calibrated molecular phylogeny of the

497 precious corals: reconciling discrepancies in the taxonomic classification and insights into
498 their evolutionary history. BMC Evol. Biol. 12. doi:Artn 246Doi 10.1186/1471-2148-12-
499 246

500 Arnold, B., Corbett-Detig, R.B., Hartl, D., Bomblies, K., 2013. RADseq underestimates diversity
501 and introduces genealogical biases due to nonrandom haplotype sampling. Mol. Ecol. 22,
502 3179–3190. doi:Doi 10.1111/Mec.12276

503 Baer, C.F., Miyamoto, M.M., Denver, D.R., 2007. Mutation rate variation in multicellular
504 eukaryotes: causes and consequences. Nat. Rev. Genet. 8, 619–631. doi:Doi
505 10.1038/Nrg2158

506 Baird, N.A., Etter, P.D., Atwood, T.S., Currey, M.C., Shiver, A.L., Lewis, Z.A., Selker, E.U.,
507 Cresko, W.A., Johnson, E.A., 2008. Rapid SNP discovery and genetic mapping using
508 sequenced RAD markers. PLoS One 3, e3376.

509 Bayer, F.M., 1956. Octocorallia, in: Moore, R.C. (Ed.), Treatise on Invertebrate Paleontology
510 Part F. Coelenterata. Geological Society of America and University of Kansas Press,
511 Lawrence, Kansas, pp. 163–231.

512 Bilewitch, J.P., Degnan, S.M., 2011. A unique horizontal gene transfer event has provided the
513 octocoral mitochondrial genome with an active mismatch repair gene that has potential for
514 an unusual self-contained function. BMC Evol. Biol. 11, 228.
515 doi:papers2://publication/doi/10.1186/1471-2148-11-228

516 Bouckaert, R., Heled, J., Kuhnert, D., Vaughan, T., Wu, C.H., Xie, D., Suchard, M.A., Rambaut,
517 A., Drummond, A.J., 2014. BEAST 2: a software platform for Bayesian evolutionary
518 analysis. PLoS Comput. Biol. 10, e1003537. doi:10.1371/journal.pcbi.1003537

519 Bouckaert, R.R., 2010. DensiTree: making sense of sets of phylogenetic trees. Bioinformatics
520 26, 1372–1373. doi:Doi 10.1093/Bioinformatics/Btq110

521 Bryant, D., Bouckaert, R., Felsenstein, J., Rosenberg, N.A., RoyChoudhury, A., 2012. Inferring
522 species trees directly from biallelic genetic markers: Bypassing gene trees in a full
523 coalescent analysis. Mol. Biol. Evol. 29, 1917–1932. doi:Doi 10.1093/Molbev/Mss086

524 Cairns, S.D., 2007. Deep-water corals: An overview with special reference to diversity and
525 distribution of deep-water scleractinian corals. Bull. Mar. Sci. 81, 311–322.

526 Cariou, M., Duret, L., Charlat, S., 2013. Is RAD-seq suitable for phylogenetic inference? An in
527 silico assessment and optimization. Ecol. Evol. 3, 846–852. doi:10.1002/ece3.512

528 Carlon, D.B., Budd, A.F., 2002. Incipient speciation across a depth gradient in a scleractinian
529 coral? Evolution (N. Y). 56, 2227–2242.

530 Catchen, J., Hohenlohe, P.A., Bassham, S., Amores, A., Cresko, W.A., 2013. Stacks: an analysis
531 tool set for population genomics. Mol. Ecol. 22, 3124–3140. doi:10.1111/Mec.12354

532 CITES, 2014. Appendices I, II and III. Convention on International Trade in Endangered Species
533 of wild fauna and flora, , http://www.cites.org/sites/default/files/eng/app/2014/E-
534 Appendices-2014-09-14.pdf.

535 Concepcion, G.T., Crepeau, M.W., Wagner, D., Kahng, S.E., Toonen, R.J., 2007. An alternative
536 to ITS, a hypervariable, single-copy nuclear intron in corals, and its use in detecting cryptic
537 species within the octocoral genus *Carijoa*. Coral reefs 27, 323–336. doi:10.1007/s00338-

538 007-0323-x

539 Cruaud, A., Gautier, M., Galan, M., Foucaud, J., Saune, L., Dubois, E., Nidelet, S., Deuve, T.,
540 Rasplus, J.-Y.J., Genson, G., Dubois, E., Nidelet, S., Deuve, T., Rasplus, J.-Y.J., 2014.
541 Empirical Assessment of RAD Sequencing for Interspecific Phylogeny. Mol. Biol. Evol. 31,
542 1272–1274. doi:10.1093/molbev/msu063

543 Darriba, D., Taboada, G.L., Doallo, R., Posada, D., 2012. jModelTest 2: more models, new
544 heuristics and parallel computing. Nat. Methods 9, 772.

545 De Queiroz, K., 2007. Species concepts and species delimitation. Syst. Biol. 56, 879–886.

546 Dueñas, L.F., Sánchez, J.A., 2009. Character lability in deep-sea bamboo corals (Octocorallia,
547 Isididae, Keratoisidinae). Mar. Ecol. Prog. Ser. 397, 11–23. doi:Doi 10.3354/Meps08307

548 Eaton, D.A., 2014. PyRAD: Assembly of de novo RADseq loci for phylogenetic analyses.
549 Bioinformatics 30, 1844–1849. doi:10.1093/bioinformatics/btu121

550 Edwards, S. V, 2009. Is a new and general theory of molecular systematics emerging? Evolution
551 (N. Y). 63, 1–19. doi:Doi 10.1111/J.1558-5646.2008.00549.X

552 Emerson, K.J., Merz, C.R., Catchen, J.M., Hohenlohe, P.A., Cresko, W.A., Bradshaw, W.E.,
553 Holzapfel, C.M., 2010. Resolving postglacial phylogeography using high-throughput
554 sequencing. Proc. Natl. Acad. Sci. U. S. A. 107, 16196–16200.
555 doi:10.1073/pnas.1006538107

556 Figueroa, D.F., Baco, A.R., 2015. Octocoral mitochondrial genomes provide insights into the
557 phylogenetic history of gene order rearrangements, order reversals, and cnidarian
558 phylogenetics. Genome Biol. Evol. 7, 391–409. doi:10.1093/gbe/evu286

559 France, S.C., 2007. Genetic analysis of bamboo corals (Cnidaria : Octocorallia : Isididae): Does
560 lack of colony branching distinguish Lepidisis from Keratoisis? Bull. Mar. Sci. 81, 323–
561 333.

562 Fujisawa, T., Barraclough, T.G., 2013. Delimiting species using single-locus data and the
563 generalized mixed Yule coalescent approach: A revised method and evaluation on
564 simulated data sets. Syst. Biol. 62, 707–724. doi:Doi 10.1093/Sysbio/Syt033

565 Glazier, A.E., Etter, R.J., 2014. Cryptic speciation along a bathymetric gradient. Biol. J. Linn.
566 Soc. 113, 897–913. doi:10.1111/bij.12389

567 Gonen, S., Bishop, S.C., Houston, R.D., 2015. Exploring the utility of cross-laboratory RAD-
568 sequencing datasets for phylogenetic analysis. BMC Res. Notes 8, 299.
569 doi:10.1186/s13104-015-1261-2

570 Grasshoff, M., 1979. Zur bipolaren verbreitung der oktokoralle *Paragorgia arborea* (Cnidaria:
571 Anthozoa: Scleraxonia). Senckenbergiana Maritima 11, 115–137.

572 Hebert, P.D.N., Cywinska, A., Ball, S.L., DeWaard, J.R., 2003. Biological identifications
573 through DNA barcodes. Proc. R. Soc. B-Biological Sci. 270, 313–321. doi:Doi
574 10.1098/Rspb.2002.2218

575 Hellberg, M.E., 2006. No variation and low synonymous substitution rates in coral mtDNA
576 despite high nuclear variation. BMC Evol. Biol. 6. doi:Artn 24Doi 10.1186/1471-2148-6-24

577 Herrera, S., Baco, A., Sánchez, J.A., 2010. Molecular systematics of the bubblegum coral genera
578 (Paragorgiidae, Octocorallia) and description of a new deep-sea species. Mol. Phylogenet.

579 Evol. 55, 123–135. doi:10.1016/j.ympev.2009.12.007
580 Herrera, S., Reyes-Herrera, P.H., Shank, T.M., 2015a. Predicting RAD-seq marker numbers
581 across the eukaryotic tree of life. Genome Biol. Evol. 7, 3207–3225.
582 doi:10.1093/gbe/evv210
583 Herrera, S., Shank, T.M., Sánchez, J.A., 2012. Spatial and temporal patterns of genetic variation
584 in the widespread antitropical deep-sea coral *Paragorgia arborea*. Mol. Ecol. 21, 6053–
585 6067. doi:10.1111/mec.12074
586 Herrera, S., Watanabe, H., Shank, T.M., 2015b. Evolutionary and biogeographical patterns of
587 barnacles from deep-sea hydrothermal vents. Mol. Ecol. 24, 673–689.
588 doi:10.1111/mec.13054
589 Hipp, A.L., Eaton, D.A.R., Cavender-Bares, J., Fitzek, E., Nipper, R., Manos, P.S., 2014. A
590 framework phylogeny of the american oak clade based on sequenced RAD data. PLoS One
591 9, e93975. doi:10.1371/journal.pone.0093975
592 ICES, 2013. Assessment of the list of VME indicator species and elements. International
593 Council for the Exploration of the Sea,
594 http://www.ices.dk/sites/pub/Publication%20Reports/Advice/2013/Special%20requests/NE
595 AFC_VME_%20indicator_%20species_%20and_elements.pdf.
596 Jennings, R.M., Etter, R.J., Ficarra, L., 2013. Population differentiation and species formation in
597 the deep sea: the potential role of environmental gradients and depth. PLoS One 8, e77594.
598 doi:10.1371/journal.pone.0077594
599 Kass, R.E., Raftery, A.E., 1995. Bayes Factors. J. Am. Stat. Assoc. 90, 773–795.
600 Kükenthal, W., 1916. System und Stammesgeschichte der Scleraxonier und der Ursprung der
601 Holaxonier. Zool. Anz. 47, 170–183.
602 Leaché, A.D., Banbury, B.L., Felsenstein, J., de Oca, A. nieto-M., Stamatakis, A., 2015. Short
603 Tree, Long Tree, Right Tree, Wrong Tree: New Acquisition Bias Corrections for Inferring
604 SNP Phylogenies. Syst. Biol. 64, syv053. doi:10.1093/sysbio/syv053
605 Leaché, A.D., Fujita, M.K., Minin, V.N., Bouckaert, R.R., 2014. Species delimitation using
606 genome-wide SNP Data. Syst. Biol. 63, 534–542. doi:10.1093/sysbio/syu018
607 Leffler, E.M., Bullaughey, K., Matute, D.R., Meyer, W.K., Segurel, L., Venkat, A., Andolfatto,
608 P., Przeworski, M., 2012. Revisiting an old riddle: What determines genetic diversity levels
609 within species? Plos Biol. 10, e1001388. doi:Artn E1001388Doi
610 10.1371/Journal.Pbio.1001388
611 Maddison, W.P., 1997. Gene trees in species trees. Syst. Biol. 46, 523–536. doi:Doi
612 10.2307/2413694
613 Mayr, E., 1942. Systematics and the Origin of Species from the Viewpoint of a Zoologist,
614 Columbia biological series. Columbia University Press, New York,.
615 McFadden, C.S., Adden, C.S., Benayahu, Y., Pante, E., Thoma, J.N., Nevarez, P.A., France,
616 S.C., 2010a. Limitations of mitochondrial gene barcoding in Octocorallia. Mol. Ecol.
617 Resour. 11, 19–31. doi:10.1111/j.1755-0998.2010.02875.x
618 McFadden, C.S., France, S.C., Sánchez, J.A., Alderslade, P., 2006. A molecular phylogenetic
619 analysis of the Octocorallia (Cnidaria: Anthozoa) based on mitochondrial protein-coding

sequences. Mol. Phylogenet. Evol. 41, 513–527.

McFadden, C.S., Sánchez, J.A., France, S.C., 2010b. Molecular Phylogenetic Insights into the Evolution of Octocorallia: A Review. Integr. Comp. Biol. 50, 389–410. doi:10.1093/icb/icq056

McFadden, C.S., van Ofwegen, L.P., 2013. Molecular phylogenetic evidence supports a new family of octocorals and a new genus of Alcyoniidae (Octocorallia, Alcyonacea). Zookeys 346, 59–83. doi:Doi 10.3897/Zookeys.346.6270

Miller, K.J., Rowden, A.A., Williams, A., Haussermann, V., 2011. Out of their depth? Isolated deep populations of the cosmopolitan coral *Desmophyllum dianthus* may be highly vulnerable to environmental change. PLoS One 6, e19004. doi:papers2://publication/doi/10.1371/journal.pone.0019004.t004

Morrison, C.L., Ross, S.W., Nizinski, M.S., Brooke, S., Jarnegren, J., Waller, R.G., Johnson, R.L., King, T.L., 2011. Genetic discontinuity among regional populations of *Lophelia pertusa* in the North Atlantic Ocean. Conserv. Genet. 12, 713–729. doi:DOI 10.1007/s10592-010-0178-5

Pante, E., Abdelkrim, J., Viricel, A., Gey, D., France, S.C., Boisselier, M.C., Samadi, S., 2014. Use of RAD sequencing for delimiting species. Heredity (Edinb). 114, 450–459. doi:10.1038/hdy.2014.105

Park, E., Hwang, D.S., Lee, J.S., Song, J.I., Seo, T.K., Won, Y.J., 2012. Estimation of divergence times in cnidarian evolution based on mitochondrial protein-coding genes and the fossil record. Mol. Phylogenet. Evol. 62, 329–345. doi:Doi 10.1016/J.Ympev.2011.10.008

Prada, C., Hellberg, M.E., 2013. Long prereproductive selection and divergence by depth in a Caribbean candelabrum coral. Proc. Natl. Acad. Sci. U. S. A. 110, 3961–3966. doi:10.1073/pnas.1208931110

Quattrini, A.M., Baums, I.B., Shank, T.M., Morrison, C.L., Cordes, E.E., 2015. Testing the depth-differentiation hypothesis in a deepwater octocoral. Proc. Biol. Sci. 282, 20150008. doi:10.1098/rspb.2015.0008

Quattrini, A.M., Georgian, S.E., Byrnes, L., Stevens, A., Falco, R., Cordes, E.E., 2013. Niche divergence by deep-sea octocorals in the genus *Callogorgia* across the continental slope of the Gulf of Mexico. Mol. Ecol. 22, 4123–4140. doi:10.1111/mec.12370

Rambaut, A., Drummond, A.J., 2007. Tracer v1.4, Available from http://beast.bio.ed.ac.uk/Tracer.

Reitzel, A.M., Herrera, S., Layden, M.J., Martindale, M.Q., Shank, T.M., 2013. Going where traditional markers have not gone before: Utility of and promise for RAD sequencing in marine invertebrate phylogeography and population genomics. Mol. Ecol. 22, 2953–2960. doi:10.1111/mec.12228

Roberts, J.M., Wheeler, A., Freiwald, A.R., Cairns, S.D., 2009. Cold-Water Corals : The Biology and Geology of Deep-Sea Coral Habitats. Cambridge University Press, Cambridge, UK ; New York.

Rubin, B.E., Ree, R.H., Moreau, C.S., 2012. Inferring phylogenies from RAD sequence data. PLoS One 7, e33394. doi:10.1371/journal.pone.0033394

662 Sánchez, J.A., 2005. Systematics of the bubblegum corals (Cnidaria: Octocorallia:
663 Paragorgiidae) with description of new species from New Zealand and the Eastern Pacific.
664 Zootaxa 1014, 1–72. doi:papers2://publication/uuid/C9A26ACD-0C36-46DC-834A-
665 68449F6B83B8

666 Sánchez, J.A., Dorado, D., 2008. Intragenomic ITS2 variation in Caribbean seafans. Proc. 11th
667 Int. Coral Reef Symp.

668 Shearer, T.L., Van Oppen, M.J.H., Romano, S.L., Worheide, G., 2002. Slow mitochondrial DNA
669 sequence evolution in the Anthozoa (Cnidaria). Mol. Ecol. 11, 2475–2487. doi:Doi
670 10.1046/J.1365-294x.2002.01652.X

671 Stamatakis, A., 2014. RAxML version 8: A tool for phylogenetic analysis and post-analysis of
672 large phylogenies. Bioinformatics 30, 1312–1313. doi:10.1093/bioinformatics/btu033

673 Stiasny, G., 1937. Die Gorgonacea der Siboga-Expedition. Supplement II, Revision der
674 Scleraxonia mit ausschluss der Melitodidae und Coralliidae. Siboga-Expedition Monogr.
675 13b, 1–138.

676 Uda, K., Komeda, Y., Fujita, T., Iwasaki, N., Bavestrello, G., Giovine, M., Cattaneo-Vietti, R.,
677 Suzuki, T., 2013. Complete mitochondrial genomes of the Japanese pink coral (*Corallium*
678 *elatius*) and the Mediterranean red coral (*Corallium rubrum*): a reevaluation of the
679 phylogeny of the family Coralliidae based on molecular data. Comp. Biochem. Physiol. D-
680 Genomics Proteomics 8, 209–219. doi:Doi 10.1016/J.Cbd.2013.05.003

681 Verrill, A.E., 1922. Part G: Alcyonaria and Actiniaria. Rep. Can. Arct. Exped. 1913-18 8, 1–164.

682 Wagner, C.E., Keller, I., Wittwer, S., Selz, O.M., Mwaiko, S., Greuter, L., Sivasundar, A.,
683 Seehausen, O., 2012. Genome-wide RAD sequence data provide unprecedented resolution
684 of species boundaries and relationships in the Lake Victoria cichlid adaptive radiation. Mol.
685 Ecol. 22, 787–798. doi:10.1111/mec.12023

686 Watling, L., France, S.C., Pante, E., Simpson, A., 2011. Biology of Deep-Water Octocorals,
687 Advances in Marine Biology. doi:10.1016/B978-0-12-385529-9.00002-0

688 Yang, Z.H., Rannala, B., 2010. Bayesian species delimitation using multilocus sequence data.
689 Proc. Natl. Acad. Sci. U. S. A. 107, 9264–9269. doi:Doi 10.1073/Pnas.0913022107

690 Zapata, F., Jimenez, I., 2012. Species delimitation: Inferring gaps in morphology across
691 geography. Syst. Biol. 61, 179–194. doi:Doi 10.1093/Sysbio/Syr084

692 Zhang, J., Kapli, P., Pavlidis, P., Stamatakis, A., 2013. A general species delimitation method
693 with applications to phylogenetic placements. Bioinformatics 29, 2869–2876.
694 doi:10.1093/bioinformatics/btt499

695

696 **Figure captions**

697

698 **Figure 1.** Proportion of loci shared among individuals of the AC clade in the optimal **backbone**
699 matrix (c 0.80, m 9). Each family is indicated with a different colour: red for Paragorgiidae; blue
700 for Coralliidae; and yellow for Alcyoniidae. Black-filled circles represent the proportion of the
701 total number of loci shared among individuals. Red-filled circles represent the proportion of the
702 total number of loci present in each individual. Circle scale shows the number of loci represented

by 100% and 50% circle sizes. Grey vertical bars represent the average proportion of loci shared by each individual. Phylogenetic tree was inferred with RAxML. All branches have bootstrap support of 100 except for those shown. This figure was generated with the package RADami (Hipp et al., 2014).

Figure 2. Phylogenetic trees of the AC clade based on RAD-seq and mitochondrial data. Left tree based on the RAD-seq concatenated **PHYLO** supermatrix (5,997 loci that contained data for at least 75% of the specimens; 85,293 variable sites; 53,150 of which were phylogenetically-informative). Right tree based on the *mtMutS* **mitochondrial** matrix (711 bp, 130 variable sites, 101 informative). Each family is indicated with a different branch colour: blue red for Paragorgiidae; blue for Coralliidae; and yellow for Alcyoniidae. Phylogenetic trees were inferred with RAxML. Branch labels indicate bootstrap support values greater than 50; * indicates support of 100. Scale bar indicates substitutions per site.

Figure 3. Species delineation hypotheses for *Paragorgia.* Schematic shows the different species delimitation models for *Paragorgia* evaluated with the BFD* method and their results. *Sibogagorgia* was included as outgroup to root the inferences for *Paragorgia*. The first model (**morphid**) indicates the species identifications based on morphology. For all models, numbered groupings indicate the species assignments. Bottom rows show the total number of species proposed, the marginal likelihood estimate (calculated on the supermatrix **PARAGORGIA,** which contains 1,203 SNPs present in all individuals), rank for each model, and Bayes Factor comparisons [2log10(BF), calculated with respect to the null **morphid** model]. Phylogenetic tree on the left, shown only for visual reference, was inferred with the RAD-seq concatenated PARAGORGIID matrix in RAxML. Branch labels indicate bootstrap support values greater than 50; * indicates support of 100. Scale bar indicates substitutions per site.

Figure 4. Species tree of *Paragorgia.* This claudogram illustrates the posterior distribution of species trees inferred with SNAPP based on the best species delimitation model PABSTE. High colour density is indicative of areas in the species trees with high topology agreement. Different colours represent different topologies. The maximum clade credibility species tree is shown with thicker branches. Trees with the same topology as the maximum clade credibility species tree are coloured in red. Trees with different topologies are coloured green or blue. With the exception of the branch leading to the clade of *P. johnsoni, P. maunga*, and *P. alisonae,* which has a posterior probability of 0.87, all interior branches have posterior probabilities of 1.0.

Figure 5. *Paragorgia jamesi* sp. nov. type specimens. A-F, Holotype RBCM 010-00234-004; A, cross section of a terminal branch; B, whole specimen (photos courtesy of Heidi Gartner); C, typical polyp sclerite; D-E, 7- and 8-radiate surface sclerites; F, medulla sclerites. G-K, Paratype USNM 1007316; G, whole specimen (photo courtesy of Robert Ford and Stephen Cairns); H, typical polyp sclerites; I-J, 7- and 8-radiate surface sclerites; K, medulla sclerites. Scale bars for C-F and H-K are 20 μm.

Figure 6. *Paragorgia stephencairnsi* representative examined material. A-C, USNM 1157074; A, typical polyp sclerites; B, 7- and 8-radiate surface sclerites; C, medulla sclerites. D-F, WHOI C03; D, typical polyp sclerites; E, 7- and 8-radiate surface sclerites; F, medulla sclerites. All all scale bars are 20 μm.

Figure 1

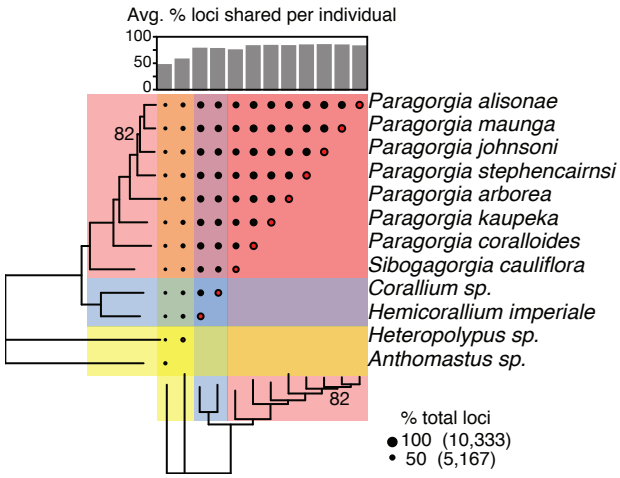
Avg. % loci shared per individual
100
50
0
82
Paragorgia alisonae
Paragorgia maunga
Paragorgia johnsoni
Paragorgia stephencairnsi
Paragorgia arborea
Paragorgia kaupeka
Paragorgia coralloides
Sibogagorgia cauliflora
Corallium sp.
Hemicorallium imperiale
Heteropolypus sp.
Anthomastus sp.
82
% total loci
100 (10,333)
50 (5,167)

Figure 2

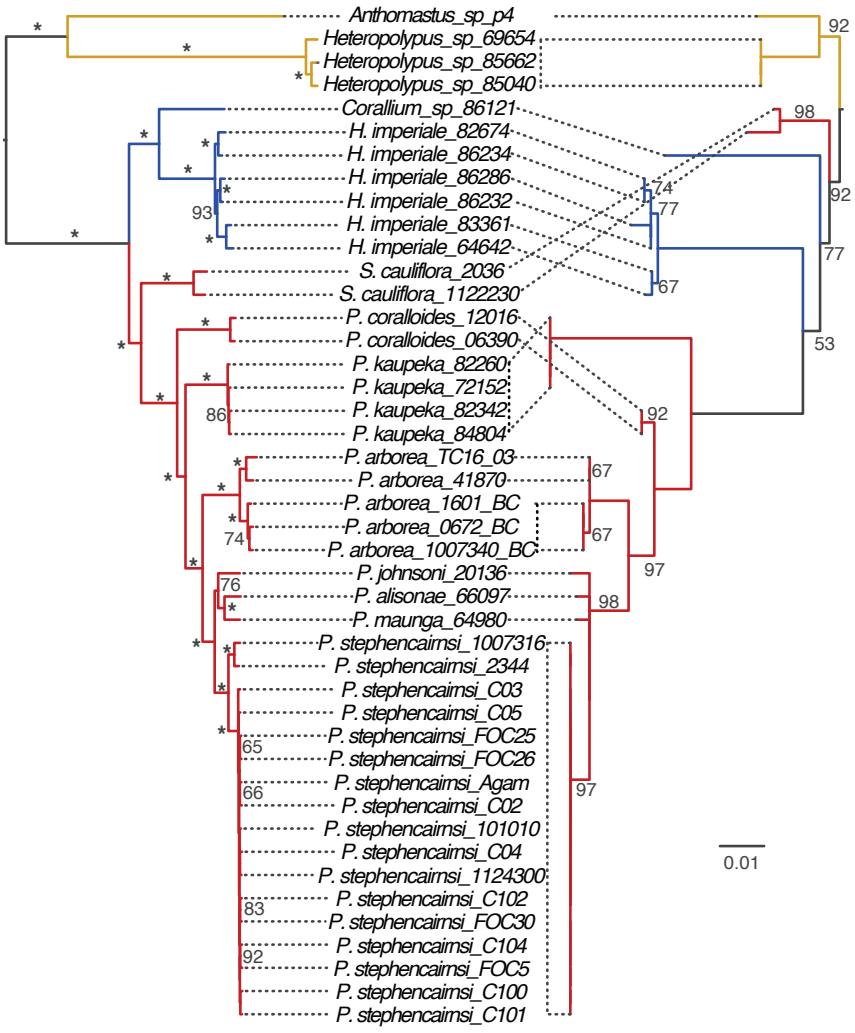
Anthomastus_sp_p4
Heteropolypus_sp_69654
Heteropolypus_sp_85662
Heteropolypus_sp_85040
Corallium_sp_86121
H. imperiale_82674
H. imperiale_86234
H. imperiale_86286
H. imperiale_86232
H. imperiale_83361
H. imperiale_64642
S. cauliflora_2036
S. cauliflora_1122230
P. coralloides_12016
P. coralloides_06390
P. kaupeka_82260
P. kaupeka_72152
P. kaupeka_82342
P. kaupeka_84804
P. arborea_TC16_03
P. arborea_41870
P. arborea_1601_BC
P. arborea_0672_BC
P. arborea_1007340_BC
P. johnsoni_20136
P. alisonae_66097
P. maunga_64980
P. stephencairnsi_1007316
P. stephencairnsi_2344
P. stephencairnsi_C03
P. stephencairnsi_C05
P. stephencairnsi_FOC25
P. stephencairnsi_FOC26
P. stephencairnsi_Agam
P. stephencairnsi_C02
P. stephencairnsi_101010
P. stephencairnsi_C04
P. stephencairnsi_1124300
P. stephencairnsi_C102
P. stephencairnsi_FOC30
P. stephencairnsi_C104
P. stephencairnsi_FOC5
P. stephencairnsi_C100
P. stephencairnsi_C101
0.01

Figure 3

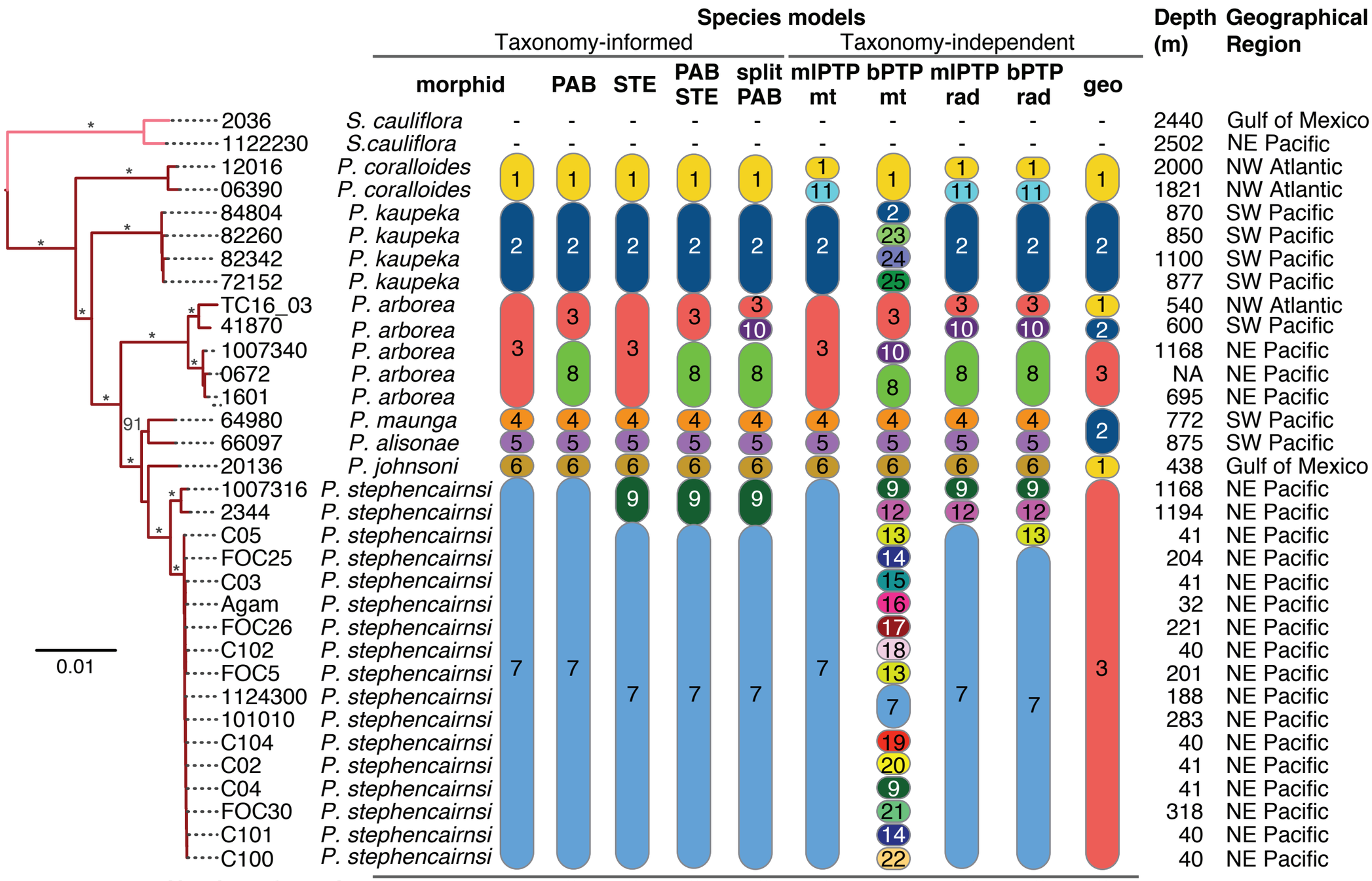
Species models
Taxonomy-informed
Taxonomy-independent
morphid
PAB
STE
PAB STE
split PAB
mlPTP mt
bPTP mt
mlPTP rad
bPTP rad
geo
Depth (m)
Geographical Region
2036 S. cauliflora - - - - - - - - - - 2440 Gulf of Mexico
1122230 S.cauliflora - - - - - - - - - - 2502 NE Pacific
12016 P. coralloides 1 1 1 1 1 1 1 1 1 1 2000 NW Atlantic
06390 P. coralloides 11 1 11 11 1821 NW Atlantic
84804 P. kaupeka 2 870 SW Pacific
82260 P. kaupeka 2 2 2 2 2 2 23 2 2 2 850 SW Pacific
82342 P. kaupeka 24 1100 SW Pacific
72152 P. kaupeka 25 877 SW Pacific
TC16_03 P. arborea 3 3 3 3 3 3 3 3 1 540 NW Atlantic
41870 P. arborea 10 3 10 10 2 600 SW Pacific
1007340 P. arborea 3 3 3 3 10 1168 NE Pacific
0672 P. arborea 8 8 8 8 8 NA NE Pacific
1601 P. arborea 8 3 695 NE Pacific
64980 P. maunga 4 4 4 4 4 4 4 4 4 2 772 SW Pacific
66097 P. alisonae 5 5 5 5 5 5 5 5 5 875 SW Pacific
20136 P. johnsoni 6 6 6 6 6 6 6 6 6 1 438 Gulf of Mexico
1007316 P. stephencairnsi 9 9 9 9 9 9 9 9 1168 NE Pacific
2344 P. stephencairnsi 12 12 12 1194 NE Pacific
C05 P. stephencairnsi 13 13 41 NE Pacific
FOC25 P. stephencairnsi 14 204 NE Pacific
C03 P. stephencairnsi 15 41 NE Pacific
Agam P. stephencairnsi 16 32 NE Pacific
FOC26 P. stephencairnsi 17 221 NE Pacific
C102 P. stephencairnsi 18 40 NE Pacific
FOC5 P. stephencairnsi 7 7 7 7 7 7 13 7 7 3 201 NE Pacific
1124300 P. stephencairnsi 7 7 7 188 NE Pacific
101010 P. stephencairnsi 283 NE Pacific
C104 P. stephencairnsi 19 40 NE Pacific
C02 P. stephencairnsi 20 41 NE Pacific
C04 P. stephencairnsi 9 41 NE Pacific
FOC30 P. stephencairnsi 21 318 NE Pacific
C101 P. stephencairnsi 14 40 NE Pacific
C100 P. stephencairnsi 22 40 NE Pacific
91
0.01
Number of species 7 8 8 9 10 8 24 12 13 3
Marginal Likelihood -6240 -6221 -6039 -6014 -6028 -6251 -6243 -6050 -6045 -10296
Rank 7 6 3 1 2 9 8 5 4 10
2log(Bayes Factor) - -38 -401 -451 -424 23 7 -379 -388 8113

Figure 4

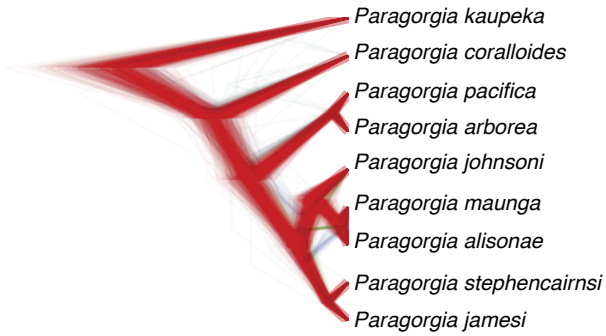
Paragorgia kaupeka
Paragorgia coralloides
Paragorgia pacifica
Paragorgia arborea
Paragorgia johnsoni
Paragorgia maunga
Paragorgia alisonae
Paragorgia stephencairnsi
Paragorgia jamesi

Figure 5

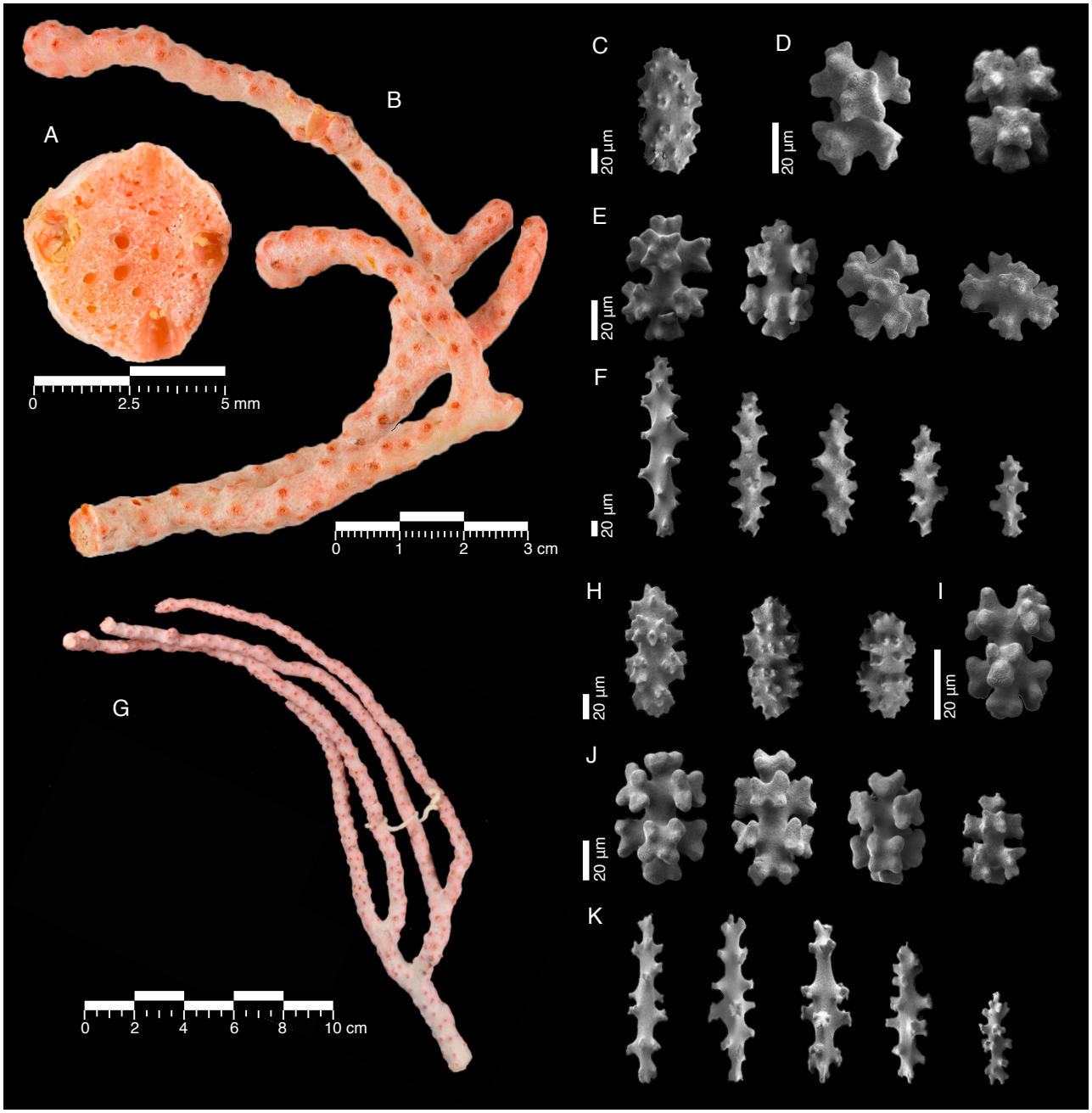

Figure 6

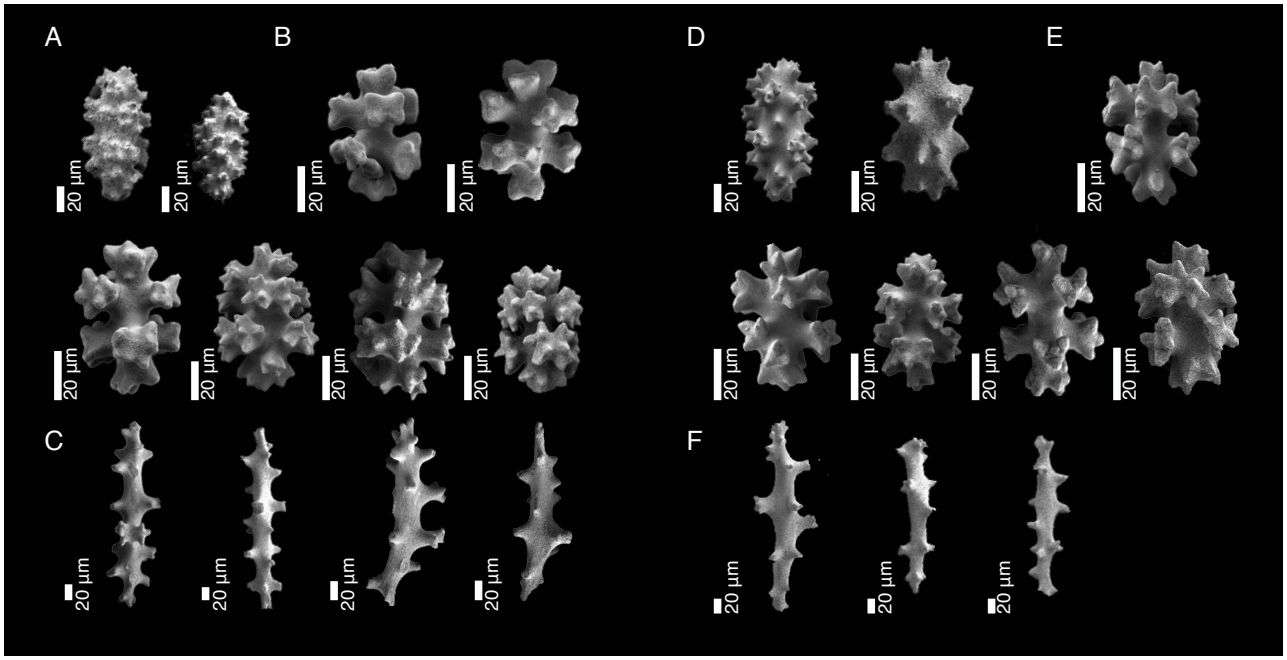

Graphical Abstract

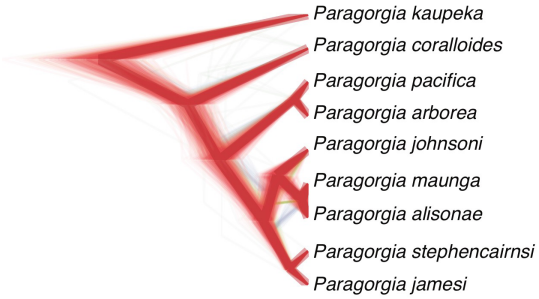

Image courtesy of NOAA Okeanos Explorer Program, 2013 Northeast U.S. Canyons Expedition